From Rigid to Flexible: Solution-Processed Carbon Nanotube Deposition on Polymeric Substrates for the Fabrication of Transistor-Based Ion Sensors

Mattia Petrelli, *Graduate Student Member, IEEE*, Bajramshahe Shkodra, Aniello Falco, Martina Aurora Costa Angeli, *Member, IEEE*, Sahira Vasquez, Antonio Orlando, Alessandra Scarton, Silvia Pogliaghi, Roberto Biasi, Paolo Lugli, *Fellow, IEEE*, and Luisa Petti, *Senior Member, IEEE*

***Abstract*— Electrolyte-gated field-effect transistors (EG-FETs) are widely used in the growing field of biochemical sensing applications, due to their manifold advantages, such as large specific capacitance, low operating voltage, and intrinsic signal amplification. In this work, carbon nanotube (CNT) EG-FET (EG-CNTFET)-based sensors for ammonium (NH_4^+) detection are reported. The active semiconducting single-walled CNTs layer was manufactured through a cost-effective and scalable spray deposition technique. To achieve high-quality semiconducting networks, the CNT ink was optimized. Atomic force microscopy (AFM) analysis was used to optimize the CNT concentration and significantly reduce the posttreatment time from the previously reported 12 to 1 h. The optimized ink was then used to fabricate EG-CNTFETs first on standard rigid Si/SiO_2 substrate and then on flexible polyimide (PI) foils. Both devices showed typical p-type behavior with an on–off ratio in the order of magnitude of 1×10^3 A/A. Furthermore, as proof of concept, we demonstrated the detection of the NH_4^+ ions with EG-CNTFETs fabricated on a flexible substrate and functionalized with nonactin ion-selective membrane. The calibration curve of the fabricated sensors showed a linear detection range for ammonium from 0.01 to 10 mM, covering the entire range of physiological concentrations of interest, with an average sensitivity of 0.346 μA/decade and a 94.35% coefficient of determination.**

Manuscript received 26 June 2023; accepted 1 August 2023. Date of publication 7 August 2023; date of current version 4 October 2023. This work was supported in part by the Autonomous Province of Bolzano-South Tyrol's European Regional Development Fund (ERDF) Program (project codes EFRE/FESR 1068-Senslab and EFRE/FESR 1127-STEX) and in part by the Istituto Italiano di Tecnologia (IIT). An earlier version of this paper was presented at the 2022 IEEE International Flexible Electronics Technology Conference (IFETC) [DOI: 10.1109/IFETC53656.2022.9948472]. *(Mattia Petrelli and Bajramshahe Shkodra contributed equally to this work.) (Corresponding author: Mattia Petrelli.)*

Mattia Petrelli, Bajramshahe Shkodra, Aniello Falco, Martina Aurora Costa Angeli, Sahira Vasquez, Paolo Lugli, and Luisa Petti are with the Sensing Technologies Laboratory (STL), Faculty of Engineering, Free University of Bozen-Bolzano, 39100 Bozen, Italy (e-mail: mattia.petrelli@unibz.it; bajramshahe.shkodra@unibz.it).

Antonio Orlando is with the Sensing Technologies Laboratory (STL), Faculty of Engineering, Free University of Bozen-Bolzano, 39100 Bozen, Italy, and also with the MNF-Micro Nano Facility Unit, Sensors and Devices Center, Bruno Kessler Foundation, 38123 Trento, Italy.

Alessandra Scarton and Roberto Biasi are with Microgate Srl, 39100 Bozen, Italy.

Silvia Pogliaghi is with the Department of Neuroscience, Biomedicine and Movement Science, University of Verona, 37129 Verona, Italy.

This article has supplementary downloadable material available at https://doi.org/10.1109/JFLEX.2023.3303149, provided by the authors.

Digital Object Identifier 10.1109/JFLEX.2023.3303149

***Index Terms*— Biosensors, carbon nanotubes (CNTs), ion-selective membranes, planar gate, sweat sensing, wearable electronics.**

I. Introduction

ELECTROLYTE-GATED field-effect transistors (EG-FETs) have recently attracted paramount interest in the field of biosensing, thanks to several distinctive features such as superior electronic properties, intrinsic signal amplification, suitability for small-scale integration with in vitro systems, low operating voltages ($<|1|$ V) allowing operation in physiological solutions (i.e., water-based electrolytes) [1], [2], [3], [4], [5].

Among the available channel materials for EG-FETs, carbon nanotubes (CNTs) have demonstrated high potential for sensitive biosensing applications. CNTs are 1-D nanomaterials, with a diameter that varies from 0.4 to 100 nm and a length up to tens of micrometer [6]. The nanometric dimensions, comparable to the ones of the analytes of interest, and the high aspect ratio make them especially interesting for biosensing. Moreover, the large surface area offered for the immobilization of the bio-recognition elements can be exploited to achieve an enhancement of the overall biosensor sensitivity [7], [8]. Another extremely important feature is the solution processability that allows CNTs to be unobtrusively integrated into almost any type of substrate, from traditional rigid substrates (e.g., glass and Si/SiO_2), to flexible polymeric foils including, among the others, polyimide (PI) and polyethylene terephthalate (PET) [9], [10]. Furthermore, such flexible substrates facilitate the design and integration of EG-CNTFETs for example in wearable platforms of arbitrary shape.

Over the past few years, wearable sensors have become more and more widespread, thanks to the possibility to perform noninvasive and real-time monitoring of various physiological parameters (e.g., heart rate, temperature, and blood pressure). One of the most interesting sources of information for wearables is sweat, due to its richness of helpful analytes, such as metabolites, proteins, and ions. [11]. In a recent study, we developed an EG-CNTFET-based biosensor for ammonium (NH_4^+) detection, which was presented at IEEE IFETC 2022 [12]. Among the different

analytes, ammonium (NH_4^+) has recently been explored as a possible marker for the starting point of the metabolic breakdown of the proteins caused by the depletion of the carbohydrates (especially in the physiological concentrations: 0.12–2.17 mM) [13].

Here, we report our initial steps toward developing EG-CNTFET-based NH_4^+ sensors on flexible substrate. To do so, first, the fabrication process was established on standard Si/SiO_2 substrate. In fact, Si/SiO_2 represents an ideal substrate for the optimization of a fabrication process, thanks to its manifold favorable properties, such as low roughness, good wettability, mechanical, and thermal stability. The semiconducting channel was deposited through a cost-effective and scalable spray deposition technique compatible with rigid/polymeric surface coating. We focused our efforts on the preparation of the CNT ink, to achieve high-quality thin semiconducting CNT network. The fabrication process was subsequently adapted to fabricate EG-CNTFETs on flexible PI substrate.

Finally, as proof of concept, the EG-CNTFETs were functionalized with a nonactin ion-selective membrane for the detection of NH_4^+. Only the specific ions (i.e., NH_4^+) can be transported across the ion-selective membrane, hence ensuring sensitivity and selectivity [14], [15]. The fabricated sensors were tested for the detection of NH_4^+ over a range of concentrations from 0.01 to 100 mM. The calibration curve of the fabricated sensors showed a linear detection range for ammonium from 0.01 to 10 mM, with an average sensitivity of 0.346 μA/decade and a coefficient of determination of 94.35%.

II. Materials and Methods

All chemicals were purchased from Sigma-Aldrich, unless otherwise stated. All solutions and dispersions were prepared using deionized (DI) water with a resistivity of 18.2 MΩ cm produced by a Milli-Q system (Millipore, SAS, France). The main steps of the fabrication of the proposed EG-CNTFET-based sensors are depicted in Fig. 1, while an overview of each separate process is presented in the following Sections.

A. Semiconducting CNT Ink Preparation

For the preparation of the main dispersion of CNTs, 0.05%wt CNTs (95% semiconducting, catalog number 773735) were dispersed in DI water using 0.5%wt sodium carboxymethyl cellulose (CMC) as surfactant [16], [17]. The detailed description of the preparation of the CNT dispersion is given in Section 1.1 of the Supporting Information. Before the spray deposition, the CNT main dispersion was diluted in 1.3 mM CMC using different dilution ratios, for the preparation of five inks: 1:15, 1:30, 1:75, 1:150, and 1:300.

B. Electrode Fabrication

The layout of the EG-CNTFETs consists of a planar gate electrode and interdigitated electrodes (IDEs) for the source and drain (channel length L = 50 μm, channel width W = 57 mm), with an active area of 8.85 mm^2.

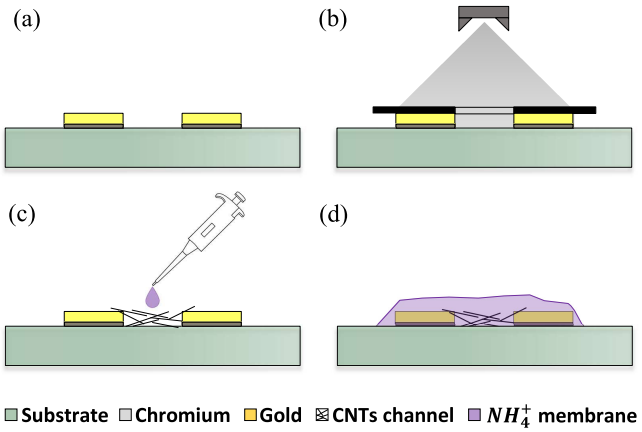

Fig. 1. Schematic representation of the electrolyte gated field-effect transistors (EG-CNTFETs) fabrication process: (a) thermally evaporated layer of 10 nm of chromium (adhesion layer) and 50 nm of gold, structured by lift off, (b) spray deposition of the semiconducting CNTs through a metallic shadow mask, employed to pattern the active area of the devices, (c) drop-casting of 10 μL of NH_4^+-selective membrane on top of the active area of the devices, and (d) schematic side-view of the obtained EG-CNTFET-based NH_4^+ sensor.

The three electrodes were patterned by one step of standard negative photolithography on Si/SiO_2 (100 nm oxide thickness, Microchemicals GmbH, Germany) or PI substrates (50 μm thickness, Kapton[1] EN, DuPont[2], USA), followed by thermal evaporation (MBRAUN ProVap 5G, equipped with an INFICON SQM-160 rate-thickness monitor) of 10 nm of chromium (Cr) and 50 nm of gold (Au). The Cr was employed as adhesion layer between the substrate and the Au.

C. Spray Deposition of the Semiconducting CNT Ink

The spray deposition was carried out by means of an automated system equipped with an industrial air atomizing spray valve (Nordson EFD 781S, USA). The experimental parameters of the spray deposition process are given in Section 1.2 of the Supporting Information. The spraying valve was programed to describe a serpentine shape above the active area of the device, to ensure homogeneous deposition of the ink. A complete cycle of the spraying valve is what is hereby defined as a "layer" of CNTs. After spraying, to remove the CMC surfactant and, at the same time, enhance the conductivity of the nanotubes (via acid doping), the devices were immersed in 2.90 M nitric acid (HNO_3) for respectively 1 , 6 , and 9 h at room temperature [18], followed by a water bath for 30 min, and a final drying step on a hot plate at 100 °C for 30 min as well. From now on, this posttreatment will be synthetically recalled as $HNO_3 + H_2O$ *treatment*.

The quality of the spray-deposited CNT layers was analyzed by atomic force microscopy (AFM) imaging (Nanosurf Core-AFM, Switzerland) after the acid posttreatment, as discussed in Section III-A.

D. EG-CNTFETs Electrical Characterization

The electrical characterization of the EG-CNTFETs was carried out by means of a probe station, connected to a

[1]Registered trademark.
[2]Trademarked.

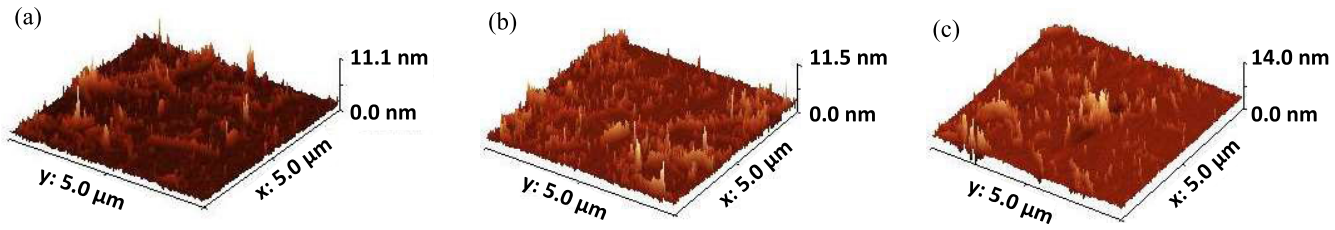

Fig. 2. Three-dimensional AFM topography of the spray-deposited CNT ink (1:30 dilution) on Si/SiO_2 after the removal of the CMC matrix through the *$HNO_3 + H_2O$ treatment* for (a) 1 h, (b) 3 h, and (c) 6 h of *$HNO_3 + H_2O$ treatment time*. The thicknesses of the three CNT random networks, reported in the z-axis scale, were similar between the three treatment times.

Keysight B1500A Semiconductor Device Parameter Analyzer. The source–drain resistance R_{DS} of the devices was measured, by sweeping the drain-source voltage V_{DS} from -0.5 to 0.5 V and measuring the drain-source current I_{DS}. The transfer characteristics were recorded by sweeping the gate-source voltage V_{GS} from 0.8 to -0.8 V, while maintaining the V_{DS} constant at -0.1 V. The output characteristics were recorded varying the V_{DS} from 0 to -0.6 V for different values of V_{GS} (from 0.2 to -0.8 V, with -0.2 V steps). The devices were then characterized in terms of threshold voltage V_{TH} and I_{ON}/I_{OFF} ratio.

E. EG-CNTFETs Functionalization

An NH_4^+-selective membrane, based on the nonactin ionophore, was employed for the functionalization of the fabricated EG-CNTFETs on flexible PI. The membrane cocktail was prepared according to the procedure reported in [19], with some modification. The details on membrane preparation and subsequent device functionalization are given in Section 1.3 of the Supporting Information. The thickness of the drop-casted NH_4^+-selective membrane was measured by means of a contact profilometer (Tencor^2 P-6 Stylus Profiler, KLA Instruments, California, USA).

F. EG-CNTFET-Based NH_4^+ Sensors Characterization

A custom-made polyethylene chamber was mounted to ensure the full coverage of the three electrodes with 200 μL of DI water. Transfer and output characteristics were recorded immediately after the addition of DI water. While the initial electrical characterization described in Section II-D provided comprehensive information on the EG-FET characteristics, not all voltages were relevant for their use as sensors. To achieve more efficient testing during the sensor characterization, the voltage ranges were narrowed down: the transfer characteristics were recorded sweeping the V_{GS} from 0.2 to -0.8 V, while maintaining the V_{DS} constant at -0.1 V, while the output characteristics were recorded varying the V_{DS} from 0 to -0.5 V for different values of V_{GS} (from 0 to -0.8 V, with -0.2 V steps). Afterward, the transfer characteristics were continuously recorded for 100 min, with 110 s interval between consecutive measurements, to let the devices stabilize. The devices were then tested as a sensor for the detection of five different NH_4^+ concentrations: 0.01, 0.1, 1, 10 and 100 mM. After the addition of each new concentration, 3 transfer curves were recorded, keeping the 110 s interval between consecutive curves. For the extraction of the calibration curve, only the last two curves were taken into account, to correctly discard the transient caused by the injection of the new NH_4^+ concentration.

III. Results

A. Optimization of the Semiconducting CNT Ink

The key aspect of a semiconducting CNT network for transistor-oriented applications is the uniformity of the dispersion, in terms of adequate coverage of the surface [20], [21] and absence of bundles (i.e., agglomerates of CNTs). The presence of bundles, in particular, can lead to the formation of conductive pathways, being the electrical behavior of such bundles mainly determined by the metallic nanotubes present in the random network. The conductivity of such pathways does not respond to the applied gate voltage, reducing thus the ability to modulate the I_{DS} by tuning the applied V_{GS}, and ultimately hindering the performance of the devices [22]. The quality of the spray-deposited CNT network can be controlled through a fine tuning of the ink composition (e.g., CNT concentration), of the process parameters of the ink preparation (e.g., power and time of sonication and centrifugation), and of the parameters of the spray deposition itself (e.g., the thickness of the deposited layer and the regime of deposition) [16].

As a first step in the optimization of the semiconducting CNT ink, we focused on the optimization of the concentration of the CNTs, using Si/SiO_2 as substrate. Starting from the main 0.05%wt dispersion, we prepared five different inks with different dilutions. Considering that the properties of the spray-deposited layer are largely determined by the choice and concentration of the surfactant [23], [24], [25], we kept the concentration of the CMC constant to 1.3 mM.

After the deposition, the CMC matrix needs to be completely removed, since the presence of the surfactant (inherently insulating) lowers the conductivity of the spray-deposited CNT network. It was previously reported that the samples need to be immersed for 12 h in the *$HNO_3 + H_2O$ treatment* to completely remove the surfactant [26]. In this work, we explored the possibility of reducing this processing time, testing three possible posttreatment times: 1, 3, and 6 h.

For this purpose, we prepared samples with different CNT inks (spray depositing eight layers of the inks) and tried

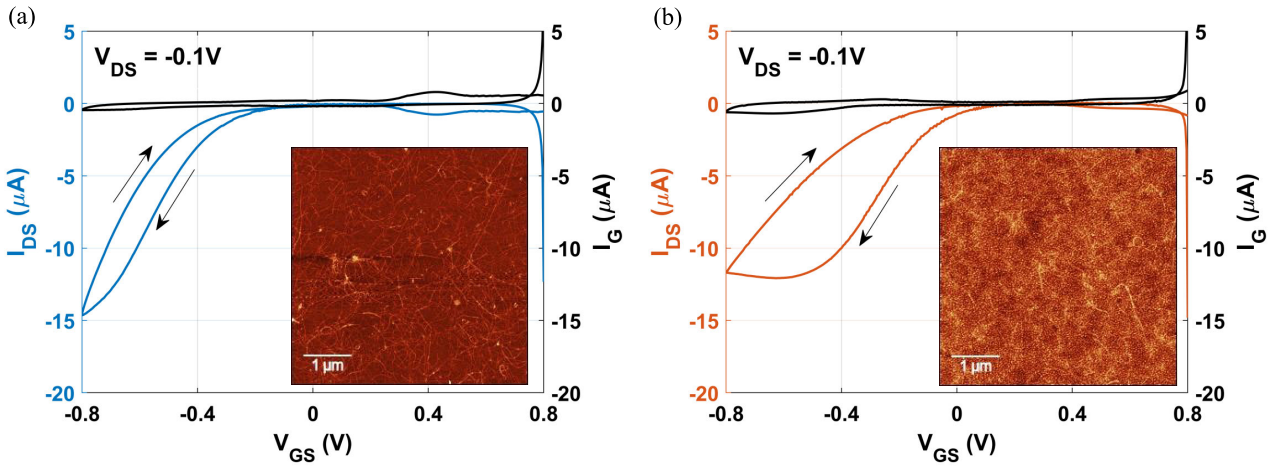

Fig. 3. Transfer characteristics for the fabricated EG-CNTFETs for (a) 18 layers of CNTs on rigid Si/SiO_2 substrate and (b) 24 layers of CNTs on flexible PI foil. Inset the 2-D AFM color map of the CNT channel, on Si/SiO_2 and PI, respectively.

different duration of the *HNO_3+H_2O treatment*. The quality of the resulting CNT network was evaluated by means of AFM microscopy. The 2-D AFM color maps are reported in the supplementary Figs. S1 (1 h treatment), S2 (3 h treatment) and S3 (6 h treatment). The CNT networks looked already completely residual-free after 1 h of *$HNO_3 + H_2O$ treatment*, as further proved by the 3-D AFM topography in Fig. 2. The thickness of the CNT layer was not affected by the time of treatment. Furthermore, Fig. S4(a) and (b) of the Supporting Information report the direct comparison of the AFM color maps before and after the *HNO_3+H_2O treatment*: the removal of the CMC matrix from the spray-deposited CNT network can be clearly observed. This is further verified from the measurement of the R_{DS}, reported in Fig. S4(c). The measured R_{DS} reduces drastically after the removal of the insulating CMC surfactant.

As expected, the density of the deposited network lowered by increasing the ratio of the dilution, as proven by the roughness values extracted from the AFM images (Table S5). The random networks deposited from the three highest dilution ratios (i.e., 1:75, 1:150, and 1:300) were characterized by very few CNTs effectively deposited on the surface. On the other hand, the CNT networks deposited from the 1:15 dilution showed the presence of CNT bundles. For this reason, the 1:30 dilution and 1 h *HNO_3 + H_2O treatment* were selected as the best CNT concentration and process parameters for the development of EG-CNTFET on rigid and flexible substrates.

B. From Rigid to Flexible Substrates

The optimized CNT ink (i.e., 1:30 dilution and 1 h of *HNO_3 + H_2O treatment*) was employed for the deposition of the channel of the EG-CNTFET fabricated on standard Si/SiO_2 substrate. We tested different number of layers of the spray-deposited CNT random networks. When depositing less than 18 layers, the devices did not show an EG-CNTFET behavior with the I_{DS} in the same range as the I_G [Fig. S6(a)]. The low conductivity of the CNT channel (R_{DS} = 107 kΩ) did not allow the formation of the required electrical double layers (EDLs), i.e., not enough ions were attracted at the interface between the semiconducting channel and the electrolyte [17]. The minimum deposition thickness allowing the targeted EG-CNTFET behavior was 18 layers, which yielded R_{DS} = 16.3 kΩ and an I_{ON}/I_{OFF} of 1.22×10^3 A/A (Fig. 3(a), with corresponding 2-D AFM color map in the inset. The corresponding semilog plot can be found in Fig. S7(a) of the Supporting Information).

To be able to integrate EG-CNTFETs in wearable platforms of arbitrary shape, it is necessary to fabricate them on conformal substrates, e.g., thin PI foil. For this reason, the fabrication process developed on the standard Si/SiO_2 substrate was adapted to the PI substrate. The EG-CNTFET fabricated on PI using the same parameters of the Si/SiO_2 device (i.e., 18 layers of CNTs) did not show the expected EG-CNTFET behavior [see Fig. S6(b)]. The measured R_{DS} was 356 kΩ, more than one order of magnitude bigger than the resistance measured on Si/SiO_2. The observed reduced channel conductivity on PI was most probably a result of the increased roughness of the polymeric surface with respect to Si/SiO_2. In fact, according to what was reported in the datasheet provided by the respective manufacturers, the root mean square (rms) roughness of the Si/SiO_2 wafer is <1 nm, while the rms roughness of the PI foil is in the 0.02–0.07 μm range. Being the rms roughness of the PI foil in the same order of magnitude of the spray-deposited CNT random networks (few tens of nanometer), more layers of material are required to overcome the substrate ridges and form a connected semiconducting path.

To obtain higher density of CNTs in the spray-deposited network, we increased the number of layers to 24. With the increased CNT density (drain–source resistance R_{DS} of 4.83 kΩ). The device fabricated on PI substrate showed typical EG-FET behavior, as shown in Fig. 3(b) (with corresponding 2-D AFM color map in the inset), with I_{ON}/I_{OFF} ratio of 2.52×10^3 A/A (the corresponding semilog plot can be found in Fig. S7(b) of the Supporting Information).

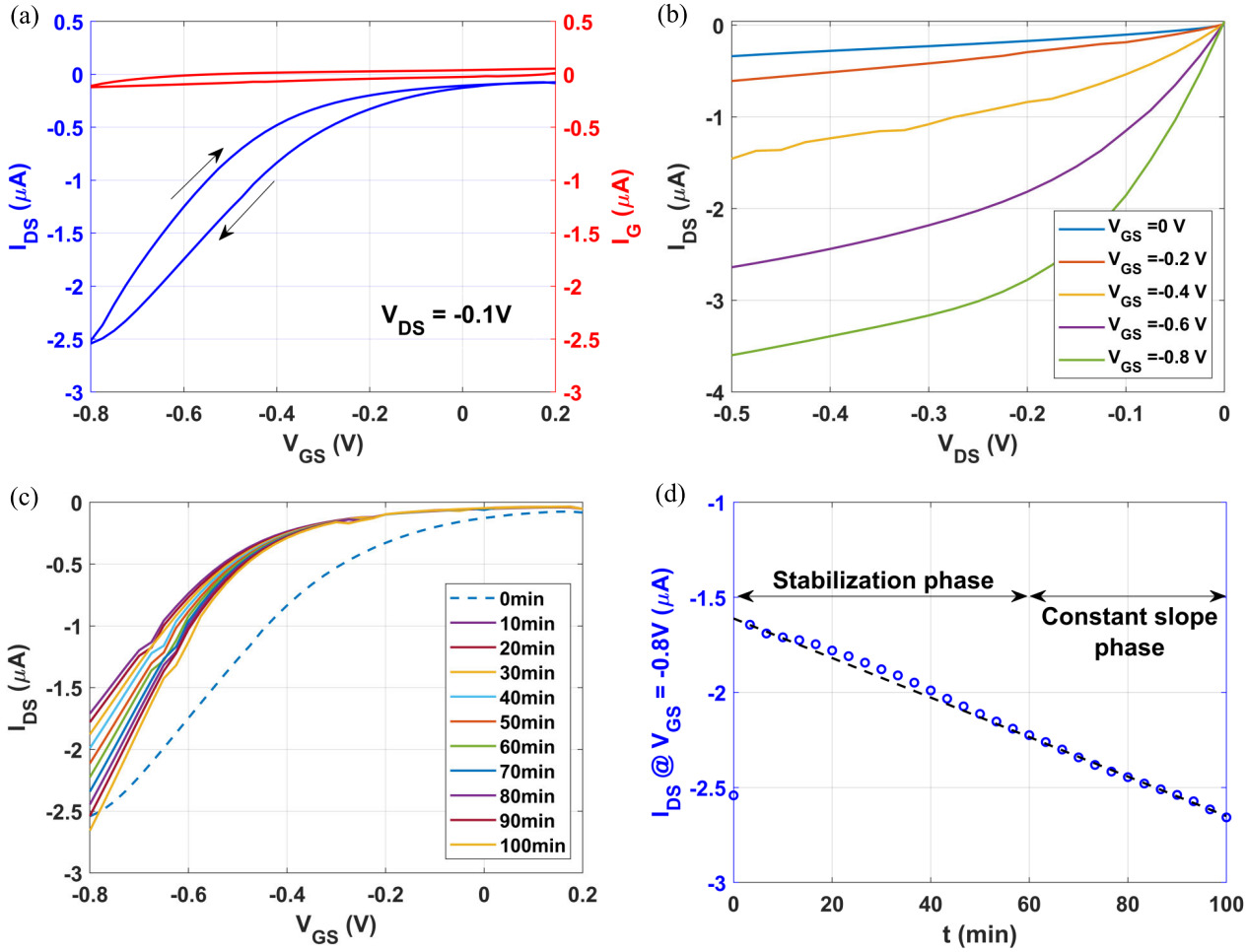

Fig. 4. (a) Transfer and (b) output characteristics of the fabricated EG-CNTFET fabricated on flexible substrate, functionalized with the NH_4^+-sensitive membrane. 200 μL of DI-water, directly drop-casted on top of the active area of the device, were used as electrolyte. The output characteristics show typical p-type behavior and absence of contact resistance. (c) Consecutive transfer characteristics recorded with only DI-water as electrolyte, to investigate the stability of the proposed EG-CNTFET-based NH_4^+ sensors. (d) Time dependence of the I_{DS} at the minimum V_{GS}, (i.e., $V_{GS} = -0.8$ V). After the stabilization phase, there is the onset of a stable linear trend that can be extracted by means of a linear fitting.

From the analysis of the transfer curves, a clear hysteresis can be observed both on rigid Si/SiO_2 and flexible PI substrate. Hysteresis can be originated either by charge transfer into the semiconducting layer from neighboring adsorbates or charge injection into trap sites on the dielectric substrate, as discussed by Wang et al. [27]. However, a proper analysis of this phenomenon would require a dedicated set of experiments, going thus beyond the scope of this article.

C. *EG-CNTFET-Based* NH_4^+ *Sensors*

Having successfully transferred the fabrication process from Si/SiO_2 to PI, we fabricated a new batch of devices (N = 3 devices), and we functionalized them by means of an NH_4^+-selective membrane to test them as NH_4^+ sensors. The thickness of the drop-casted NH_4^+-selective membrane was of 5.06 μm, with a standard deviation of 0.99 μm. A representative profilometer measurement can be observed in Fig. S8 of the Supporting Information.

Before testing the functionalized EG-CNTFETs on PI as NH_4^+ sensors, electrical characterization was performed. It can be observed, both in Fig. 3(a) and (b), how the I_{DS} and the I_G were symmetrical for the first part of the measurement (0.8 V>V_{GS}>0.2 V, approximately). This was indicative of the very early stages of the onset of the EDLs at the semiconductor-electrolyte and gate-electrolyte interfaces: until enough ions rearranged under the influence of the V_{GS} the current passed through the electrolyte. For this reason, we changed the characterization procedure, starting the sweep of the V_{GS} from 0.2 V and adding a brief hold time (i.e., the time during which the bias is applied to the device before starting the sweep) of 5 s to help the formation of the EDLs.

The transfer and output characteristics recorded in DI water showed typical p-type behavior [Fig. 4(a), with the corresponding semilog plot depicted in Fig. S9(a) of the Supporting Information, and 4(b)]. Comparing the recorded transfer curves with the ones of the bare devices [i.e., Fig. 3(b)], a clear decrease in the I_{DS} can be observed. This is to be ascribed to the penetration of the polymeric membrane, inherently insulating, into the CNT network, with the consequent reduction of the number of semiconducting paths and the overall reduction of the network conductivity, which is in turn reflected in a decrease of the I_{ON}. Moreover, the output characteristics proved the formation of stable ohmic contacts between the gold IDEs and the CNTs [28], [29].

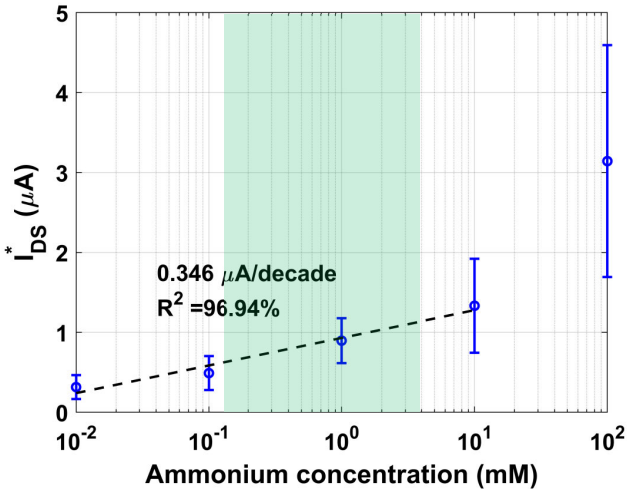

Fig. 5. Calibration curves representing the average corrected response of the EG-CNTFET-based sensors (I^*_{DS}) versus different concentrations of NH_4^+. All the devices were tested using DI water as electrolyte. The green box highlights the physiological range of concentrations of NH_4^+ during physical exercise [13]. The response of the devices toward NH_4^+ diverged from linearity when the highest concentration (100 mM) was tested, showing signs of saturation. This concentration was hence excluded from the calculation of the sensitivity. Here, the error bars represent the standard errors of the mean, with N = 3 devices.

When employing EG-CNTFETs for biosensing applications, it is crucial to assess the device stability to have reliable biosensing data [30]. Therefore, transfer characteristics were recorded for 100 min (Fig. 4(c), with the corresponding semilog plot depicted in Fig. S9(b) of the Supporting Information) prior to the exposure to the target analyte NH_4^+.

The response of devices (i.e., the value of the I_{DS} at $V_{GS} = -0.8$ V) stabilized after 1 h of measurements [Fig. 4(d)], similar to what reported in [31]. After 1 h, i.e., after the stabilization phase, the I_{DS} showed a linear increase (i.e., constant slope phase) of 10.4 nA/min, with a coefficient of determination of 99.75%. During the same time interval, the gate current I_G went through a similar stabilization, probably due to the continuous dynamic re-arrangement of the ions in the electrolyte in response to the applied V_{GS}. Nevertheless, I_G was <10 nA (in absolute value) during the whole measurement time, so at least three orders of magnitude lower than the I_{DS}, proving reliable EG-CNTFET operation of the tested devices [1]. The onset of the constant slope phase, and the possibility to extract the trend of the I_{DS} for each device by means of a linear fitting, enabled the possibility to subtract such trend and obtain the corrected response I^*_{DS} [32].

Different NH_4^+ concentrations were injected at the end of the constant slope phase. As shown in Fig. 5, exposure of the sensor to NH_4^+ led to concentration-dependent changes in I^*_{DS}: the I^*_{DS} increased for increasing concentrations of NH_4^+. Such behavior was likely driven by the ability of the ion-selective membrane to exchange the NH_4^+ ions of the electrolyte (a representative plot of the I^*_{DS} in real time can be found in Fig. S10 of the Supporting Information). The build-up of positive NH_4^+ ions inside the membrane, together with the corresponding increase in negative charge in the electrolyte (i.e., the depletion of positive charge) leads to the onset of an electrical potential difference across the membrane. This established potential difference causes a reduction in the conductivity of the semiconducting channel [33]. The response of all the tested EG-CNTFET-based NH_4^+ sensors was linear for concentrations up to 10 mM, with a sensitivity of 0.346 μA/decade (relative standard deviation of 69.2%) and a coefficient of determination of 94.35%. The response diverged from this linear behavior when 100 mM NH_4^+ was tested, the reason for this can be the saturation of the sensor: when the available sites of the nonactine ionophore inside the membrane are fully occupied by NH_4^+, the remaining free NH_4^+ cations react only electrostatically with the membrane in close proximity of the channel. This interaction, being regulated by the randomly distributed the NH_4^+ cations inside the solution, is intrinsically chaotic, leading to an increase in the standard error.

IV. Conclusion

In this work, we presented the fabrication and characterization of EG-CNTFETs on rigid and flexible substrate. The semiconducting channel was made of solution-processed CNTs and deposited through cost-effective and scalable spray deposition technique. To achieve high-quality semiconducting nanotube networks, we focused on the optimization of the CNT ink. We chose the optimal CNT concentration and significantly reduced posttreatment time from the previously reported 12 to 1 h. The optimized ink was then used to fabricate EG-CNTFET first on standard rigid Si/SiO_2 substrate and later on flexible PI foil. Both devices showed typical p-type behavior with an on-off ratio in the order of magnitude of 10^3 A/A. Furthermore, as a proof of concept, we demonstrated the detection of the NH_4^+ ions with EG-CNTFETs functionalized with nonactin ion-selective membrane. To have reliable sensing data, the sensor stability was thoroughly investigated, and a facile data analysis protocol was established. The sensors reached stability after 1 h of continuous transfer characteristics recording, which allowed for the baseline correction of the I_{DS}. Upon reaching stability, sensors were tested for the detection of NH_4^+ over the range of concentrations from 0.01 to 100 mM. The sensors showed sensitive detection of NH_4^+ in the range of interest from 0.01 to 10 mM with average sensitivities of 0.346 μA/decade and 94.35% coefficient of determination. Future work will involve the characterization with a narrower range of concentrations, possibly increasing the number of concentrations tested inside the physiological range from 0.12 to 2.17 mM, as well as performing the characterization with more complex electrolytes (i.e., artificial sweat), to explore the selectivity (i.e., the effect of interfering ions on the sensor response) [32], [34]. Another aspect that needs to be studied is the re-usability of the sensor, by studying possible mechanisms to induce recovery of the membrane after exposure to NH_4^+. The results shown in this work demonstrate the potential of using EG-CNTFETs fabricated on a flexible substrate, functionalized with nonactine-based membrane, opening a pathway for the development of a wearable platform.

References

[1] B. Shkodra et al., "Electrolyte-gated carbon nanotube field-effect transistor-based biosensors: Principles and applications," *Appl. Phys. Rev.*, vol. 8, no. 4, 2021, Art. no. 041325.

[2] C. Zhao, T. Man, Y. Cao, P. S. Weiss, H. G. Monbouquette, and A. M. Andrews, "Flexible and implantable polyimide aptamer-field-effect transistor biosensors," *ACS Sensors*, vol. 7, no. 12, pp. 3644–3653, 2022.
[3] G. Elli, S. Hamed, M. Petrelli, P. Ibba, M. Ciocca, P. Lugli, and L. Petti, "Field-effect transistor-based biosensors for environmental and agricultural monitoring," *Sensors*, vol. 22, no. 11, p. 4178, 2022.
[4] N. Nakatsuka et al., "Aptamer–field-effect transistors overcome debye length limitations for small-molecule sensing," *Science*, vol. 362, no. 6412, pp. 319–324, 2018.
[5] L. Suo et al., "'Water-in-salt' electrolyte enables high-voltage aqueous lithium-ion chemistries," *Science*, vol. 350, no. 6263, pp. 938–943, 2015.
[6] L. Hu, D. S. Hecht, and G. Gruner, "Carbon nanotube thin films: Fabrication, properties, and applications," *Chem. Rev.*, vol. 110, no. 10, pp. 5790–5844, 2010.
[7] I. V. Zaporotskova, N. P. Boroznina, Y. N. Parkhomenko, and L. V. Kozhitov, "Carbon nanotubes: Sensor properties. A review," *Mod. Electron. Mater.*, vol. 2, no. 4, pp. 95–105, 2016.
[8] B. Shkodra et al., "Polymeric integration of structure-switching aptamers on transistors for histamine sensing," *Faraday Discuss.*, Jul. 2023, doi: 10.1039/D3FD00123G.
[9] M. Petrelli et al., "Novel gate electrode design for flexible planar electrolyte-gated field-effect transistor-based sensors for real-time ammonium detection," in *Proc. IEEE Sensors*, Jul. 2022, pp. 1–4.
[10] C.-S. Lee, Y. Ju, J. Kim, and T. H. Kim, "Electrochemical functionalization of single-walled carbon nanotubes with amine-terminated dendrimers encapsulating Pt nanoparticles: Toward facile field-effect transistor-based sensing platforms," *Sensors Actuators B, Chem.*, vol. 275, pp. 367–372, Aug. 2018.
[11] A. J. Bandodkar, W. J. Jeang, R. Ghaffari, and J. A. Rogers, "Wearable sensors for biochemical sweat analysis," *Annual Rev. Anal. Chem.*, vol. 12, pp. 1–22, Jun. 2019.
[12] M. Petrelli et al., "Flexible, planar, and stable electrolyte-gated carbon nanotube field-effect transistor-based sensor for ammonium detection in sweat," in *Proc. IEEE Int. Flexible Electron. Technol. Conf. (IFETC)*, Jul. 2022, pp. 1–2.
[13] E. Renner, N. Lang, B. Langenstein, M. Struck, and T. Bertsch, "Validating sweat ammonia as physiological parameter for wearable devices in sports science," in *Proc. 42nd Annu. Int. IEEE Eng. Med. Biol. Soc. (EMBC)*, Jun. 2020, pp. 4644–4647.
[14] M. Cuartero, N. Colozza, B. M. Fernández-Pérez, and G. A. Crespo, "Why ammonium detection is particularly challenging but insightful with ionophore-based potentiometric sensors—An overview of the progress in the last 20 years," *Analyst*, vol. 145, no. 9, pp. 3188–3210, 2020.
[15] B. Martínez-Haya, J. R. Avilés-Moreno, F. Gámez, G. Berden, and J. Oomens, "Preferential host-guest coordination of nonactin with ammonium and hydroxylammonium," *J. Chem. Phys.*, vol. 149, no. 22, 2018, Art. no. 225101.
[16] A. Falco, L. Cinà, G. Scarpa, P. Lugli, and A. Abdellah, "Fully-sprayed and flexible organic photodiodes with transparent carbon nanotube electrodes," *ACS Appl. Mater. Interfaces*, vol. 6, no. 13, pp. 10593–10601, 2014.
[17] B. Shkodra et al., "Optimization of the spray-deposited carbon nanotube semiconducting channel for electrolyte-gated field-effect transistor-based biosensing applications," *IEEE Sensors J.*, early access, Mar. 29, 2022, doi: 10.1109/JSEN.2022.3162706.
[18] L. Zhang, M. Rao, J. Kochupurackal, N. Mathews, Y. M. Lam, and S. G. Mhaisalkar, "Effect of nitric acid concentration on doping of thin film single-walled carbon nanotubes for electrode application in transparent, flexible dye sensitized solar cells," *MRS Online Proc. Library (OPL)*, vol. 1436, Jan. 2013, Art. no. mrss12-1436-k06–03.
[19] T. Guinovart, A. J. Bandodkar, J. R. Windmiller, F. J. Andrade, and J. Wang, "A potentiometric tattoo sensor for monitoring ammonium in sweat," *Analyst*, vol. 138, no. 22, pp. 7031–7038, 2013.
[20] H. Okimoto et al., "Tunable carbon nanotube thin-film transistors produced exclusively via inkjet printing," *Adv. Mater.*, vol. 22, no. 36, pp. 3981–3986, 2010.
[21] F. Loghin et al., "Scalable spray deposition process for highly uniform and reproducible CNT-TFTS," *Flexible Printed Electron.*, vol. 1, no. 4, 2016, Art. no. 045002.
[22] T. Haeberle, F. Loghin, U. Zschieschang, H. Klauk, and P. Lugli, "Carbon nanotube thin-film transistors featuring transfer-printed metal electrodes and a thin, self-grown aluminum oxide gate dielectric," in *Proc. IEEE 15th Int. Conf. Nanotechnol. (IEEE-NANO)*, Jul. 2015, pp. 160–163.
[23] A. Abdelhalim, A. Abdellah, G. Scarpa, and P. Lugli, "Fabrication of carbon nanotube thin films on flexible substrates by spray deposition and transfer printing," *Carbon*, vol. 61, pp. 72–79, Sep. 2013.
[24] E. J. Lavernia and Y. Wu, *Spray Atomization and Deposition*. Hoboken, NJ, USA: Wiley-Blackwell, 1996.
[25] A. H. Lefebvre and V. G. McDonell, *Atomization and Sprays*. Boca Raton, FL, USA: CRC Press, 2017.
[26] F. Loghin, A. Rivadeneyra, M. Becherer, P. Lugli, and M. Bobinger, "A facile and efficient protocol for preparing residual-free single-walled carbon nanotube films for stable sensing applications," *Nanomaterials*, vol. 9, no. 3, p. 471, 2019.
[27] H. Wang, Y. Wu, C. Cong, J. Shang, and T. Yu, "Hysteresis of electronic transport in graphene transistors," *ACS Nano*, vol. 4, no. 12, pp. 7221–7228, 2010.
[28] G. Horowitz, "Interfaces in organic field-effect transistors," in *Organic Electronics*. Springer, 2010, pp. 113–153.
[29] H. Chen et al., "Aptamer-functionalized carbon nanotube field-effect transistor biosensors for Alzheimer's disease serum biomarker detection," *ACS Sensors*, vol. 7, no. 7, pp. 2075–2083, 2022.
[30] F. Torricelli et al., "Electrolyte-gated transistors for enhanced performance bioelectronics," *Nature Rev. Methods Primers*, vol. 1, no. 1, pp. 1–24, 2021.
[31] A. Molazemhosseini et al., "A rapidly stabilizing water-gated field-effect transistor based on printed single-walled carbon nanotubes for biosensing applications," *ACS Appl. Electron. Mater.*, vol. 3, no. 7, pp. 3106–3113, 2021.
[32] M. Petrelli et al., "Method for instability compensation and detection of ammonium in sweat via conformal electrolyte-gated field-effect transistors," *Organic Electron.*, vol. 122, Nov. 2023, Art. no. 106889.
[33] K. Melzer et al., "Flexible electrolyte-gated ion-selective sensors based on carbon nanotube networks," *IEEE Sensors Journal*, vol. 15, no. 6, pp. 3127–3134, Jun. 2015.
[34] M. Petrelli et al., "Flexible sensor and readout circuitry for continuous ion sensing in sweat," *IEEE Sensors Lett.*, vol. 7, no. 6, May 2023, Art. no. 5501804.

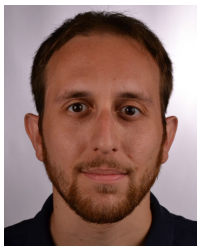

Mattia Petrelli (Graduate Student Member, IEEE) received the M.Sc. degree in electronic engineering from the University of Salerno, Fisciano, Italy, in 2017. He is currently pursuing the Ph.D. degree in advanced-systems engineering with the Free University of Bozen-Bolzano, Bozen, Italy.

His project is aimed at the design, fabrication, and characterization of real-time wearable solutions to monitor the muscles' activity, to provide immediate feedback to the athlete about their physiological status.

Bajramshahe Shkodra received the M.Sc. degree in the field of analytical and environmental chemistry from the University of Prishtina, Prishtina, Kosovo, in 2017, and the Ph.D. degree from the Free University of Bozen-Bolzano, Bozen, Italy, in 2022, working on the development of flexible and printed biosensors at the Sensing Technologies Laboratory.

Her main research interests include the design, fabrication, and characterization of biosensors for food and medical application.

Aniello Falco received the B.Sc. and M.Sc. degrees in electrical engineering from the University of Salerno, Fisciano, Italy, in 2010 and 2013, respectively, and the Ph.D. degree (Hons.) from the Technical University of Munich, Munich, Germany, in 2016, under the supervision of Prof. Paolo Lugli.

Subsequently, he joined the Institute for Nanoelectronics, Technical University of Munich, under the supervision of Prof. Paolo Lugli. In 2017, he moved to the Free University of Bozen-Bolzano, Bozen, Italy, where he collaborated until 2018 with his former supervisor to setup and develop a new research group on printed electronics. The academic experience was followed by Research and Development Project Management positions in global players in the Sensors and Semiconductors Industries, such as Alps Alpine and Infineon Technologies.

Martina Aurora Costa Angeli (Member, IEEE) received the bachelor's degree in biomedical engineering and the master's degree in biomedical biomechanics and biomaterials engineering from Politecnico di Milano, Milan, Italy, in 2013 and 2016, respectively, and the Ph.D. degree in materials engineering from Politecnico di Milano in 2020 with a thesis on the development of printed and deformable devices.

She is currently a Researcher with a fixed-term contract with the Faculty of Engineering, Free University of Bozen-Bolzano, Bozen, Italy. Her research interests include on the fabrication and characterization of chemical, physical, and wearable sensors for human monitoring.

Sahira Vasquez received the B.Sc. degree (summa cum laude) in food technology engineer from ISA University, Santiago De Los Caballeros, Dominican Republic, in 2013, and the M.Sc. degree in environmental protection and food agricultural production from Hohenheim University, Stuttgart, Germany, in 2015. She is currently pursuing the Ph.D. degree in the program food engineering and biotechnology with the Free University of Bozen-Bolzano, Bozen, Italy, where she is also working with the development of printed sensors to monitor the gases produced by the gut microbial community in an in vitro Human Microbial Ecosystem (SHIME).

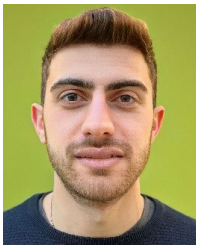

Antonio Orlando received the B.Sc. degree in chemistry from The University of Messina, Messina, Italy, in 2017, and the M.Sc. degree in chemistry, materials and energy from the University of Ferrara, Ferrara, Italy, in 2020. He is currently pursuing the Ph.D. degree in program of advanced system engineering (Inf/Ing-01) with the Free University of Bozen-Bolzano, Bozen, Italy, in collaboration with the Micro Nano Facility Group, Sensor and Device center, Bruno Kessler Foundation, Trento, Italy.

His current research interests include the investigation of innovative functional nanomaterials toward the selective detection of gaseous compounds.

Alessandra Scarton received the M.Sc. and Ph.D. degrees in bioengineering from the University of Padua, Padova, Italy, in 2012 and 2016, respectively.

She currently works as a Research and Development Engineer with Microgate Srl, Bozen, Italy. Her research interests include motion analysis in clinical and sports fields, using both mocap systems and wearable magneto-inertial sensors, biomechanical and musculoskeletal modeling of the lower limbs, and finite element analysis.

Dr. Scarton was a recipient of the Italian Society for Movement Analysis (SIAMOC) best M.Sc. thesis award in 2013, and the European Society for Movement Analysis in Clinic (ESMAC) best paper in 2016.

Silvia Pogliaghi received the M.D. degree in sports medicine from the State University of Brescia, Brescia, Italy, in 1992, and the Ph.D. degree in human physiology from the Department of Biomedical Sciences and Technologies, School of Medicine, University of Milano, Milan, Italy, in 2002.

She is currently an Associate Professor of human physiology with the University of Verona, Verona, Italy, and an Adjunct Associate Professor with the University of Western Ontario, London, ON, Canada, and the Univeristy of Calgary, Calgary, AB, Canada. She studies the physiological mechanisms that regulate and limit the acute and adaptive responses to aerobic exercise in physiological and pathological conditions. This finds a direct application in exercise prescriptions for the community.

Prof. Pogliaghi is a fellow of the American College of Sports Medicine.

Roberto Biasi received the M.Sc. degree (Hons.) in aerospace engineering from Politecnico di Milano, Milan, Italy, in 1991, and the Ph.D. degree from Politecnico di Milano in 1994 with a thesis on "Active control system for aerospace structures".

In 1989, he founds Microgate Srl. Besides the activities related to sports timing, the company deals with adaptive optics, in particular with the large contactless adaptive mirror technology currently adopted by several of the largest observatories around the world. In 2004, together with three professors, he starts Micro Photon Devices, a spin-off of Microgate and Politecnico di Milano, developing and producing single photon sensors based on the SPAD solid-state technology. His activity in science and technology is supported by more than 100 papers published in the different fields.

Paolo Lugli (Fellow, IEEE) received the degree in physics from the University of Modena and Reggio Emilia, Modena, Italy, in 1979, and the M.Sc. and Ph.D. degrees in electrical engineering from Colorado State University, Fort Collins, CO, USA, in 1982 and 1985, respectively.

He is currently a Rector with the Free University of Bozen-Bolzano, Bozen, Italy. He has authored more than 350 scientific articles.

Luisa Petti (Senior Member, IEEE) received the M.Sc. degree in electronic engineering from Politecnico di Milano, Milan, Italy, in 2011, and the Ph.D. degree in electrical engineering and information technology from ETH Zürich, Zürich, Switzerland, in 2016.

She is currently an Associate Professor with the Free University of Bozen-Bolzano, Bozen, Italy, where she researches on flexible and printed electronics for a wide range of applications, including food engineering and biotechnology.

Open Access funding provided by 'Libera Università di Bolzano' within the CRUI CARE Agreement